Proc. Natl. Acad. Sci. USA
Vol. 76, No. 4, pp. 1603–1607, April 1979
Biochemistry

^{13}C NMR studies of gluconeogenesis in rat liver cells: Utilization of labeled glycerol by cells from euthyroid and hyperthyroid rats

(pentose cycle/triiodothyronine/glycerol-3-phosphate dehydrogenase/alanine)

S. M. COHEN, S. OGAWA, AND R. G. SHULMAN

Bell Laboratories, Murray Hill, New Jersey 07974

Contributed by Robert G. Shulman, January 9, 1979

ABSTRACT **The gluconeogenic pathway from [2-^{13}C]glycerol and [1,3-^{13}C]glycerol has been followed in suspensions of isolated rat hepatocytes at 25°C by ^{13}C NMR at 90.5 MHz. The flow of label through the major pathway from glycerol to L-glycerol 3-phosphate and into glucose was followed in cells from control and triiodothyronine-treated rats. Treatment increased the rates of glucose formation and glycerol consumption 2-fold and decreased the αGP level to 40%. We calculate that ≈60% of the flux is through the mitochondrial glycerol phosphate dehydrogenase in cells from triiodothyronine-treated rats, compared with ≈15% in cells from the controls. Equal distribution of label between the trioses of glucose was obtained and, because the C_3–C_4 spin–spin coupling gives the distribution of labeled carbons in the *same* molecule, it was possible to measure the amount of triose from unlabeled fructose incorporated into the glucose labeled at carbons 1, 3, 4, and 6. About 10% of the hexoses had flowed through the pentose cycle and back into the hexose pathway in cells from fasted rats. From the distribution of label at glucose carbons not labeled via the major pathway and from the carbon spin–spin splitting patterns observed, we conclude that transketolase is reversible whereas transaldolase is essentially irreversible in the nonoxidative pentose branch.**

Recently it has become possible to study metabolism in cellular suspensions by ^{31}P (1) and ^{13}C (2) high-resolution NMR. In recent ^{31}P high-resolution NMR studies of suspensions of rat liver cells we have determined the cytosolic pH and the mitochondrial pH simultaneously from the positions of the two resolved resonances from inorganic phosphate (3). A preliminary account of ^{13}C NMR studies of intermediates and end products of gluconeogenesis in rat liver cells from a ^{13}C-labeled alanine substrate has been reported (4).

The present communication illustrates the ability of ^{13}C NMR to follow the gluconeogenic pathway from glycerol in liver cells obtained from euthyroid and hyperthyroid rats and to obtain, very simply, simultaneous quantitative measurements of the contributions of different pathways. This process has been intensively studied in perfused liver (5, 6), freeze-clamped liver (7), and isolated hepatocytes (8, 9). The early measurements by Freedland and Krebs (5) of the rate of glucose production from glycerol in perfused rat liver showed that the rate was appreciably increased in thyroxine-treated rats. Even earlier measurements by Lardy and coworkers (10) demonstrated a large increase in the rate of α-glycerophosphate oxidation by liver mitochondria from thyroid-fed rats that was due to the increased activity of the mitochondrial αGP dehydrogenase.

METHODS AND MATERIALS

Liver parenchymal cells were isolated from male Sprague–Dawley rats (190–240 g) that had been starved for 24 hr prior to sacrifice. In weight-matched groups, the animals received intraperitoneal injections of either L-3,3′,5-triiothyronine (T3; Calbiochem, B grade) dissolved in isotonic saline at pH 9.8 (T3 treated, hyperthyroid) or isotonic saline alone (euthyroid control) daily for 4 days prior to cell preparation. At the physiological dose of T3 used in these experiments, 15 μg/100 g of body weight per day, the animals showed either no weight loss or small weight gains.

The cell preparation method of Berry and Friend (11), with the modifications in the liver perfusion introduced by Williamson and coworkers (12), was used. Routinely, at least 90% of the freshly prepared cells excluded trypan blue dye and were morphologically normal under light microscopy. At the end of the typical NMR experiment of 2–3 hr duration, 70–90% of the cells were viable by these tests.

The cells were resuspended in approximately 3 times their volume of Krebs' bicarbonate medium at pH 7.4 (120 mM NaCl/24 mM $NaHCO_3$/4.8 mM KCl/1.2 mM $MgSO_4$/1.3 mM $CaCl_2$/1.2 mM KH_2PO_4) containing 25 mM 4-morpholinepropanesulfonic acid (Mops), 10% ^2H_2O, and 3% dialyzed bovine serum albumin to a final volume of 2.5 ml and a hematocrit value of 25–35%. [1,3-^{13}C]Glycerol and [2-^{13}C]glycerol (90% isotopic purity) were from Merck.

The NMR spectra were measured on a Bruker HX-360 spectrometer at 90.5 MHz for ^{13}C nuclei. All spectra were recorded at 25 ± 1°C in 10-mm-diameter tubes. Unless other conditions are specified, each ^{13}C spectrum is the Fourier transform of the accumulation of 1000 radiofrequency pulses of 60° free induction decays of 16,000 data points each, with 2-sec recovery between pulses. These NMR conditions have been determined to produce no saturation effects in the spectral regions shown here. ^{13}C chemical shifts are given relative to tetramethylsilane at 0 ppm.

For oxygenation, small quantities of 0.5 M H_2O_2 in isotonic saline were gently mixed into samples in the NMR probe at regular intervals under computer control (13). Typically 3 sec of H_2O_2 mixing was alternated with 24 sec of data accumulation.

EXPERIMENTAL RESULTS

Fig. 1*a* shows the ^{13}C NMR spectra of liver cells from a normal rat after incubation with [2-^{13}C]glycerol; the spectrum was recorded 68–105 min after the glycerol was introduced. The three spectra of Fig. 1 show only the region between 60 and 100 ppm (downfield from tetramethylsilane) which contains the glucose peaks. In order to calibrate the intensities of the different glucose peaks, Fig. 1*b* shows a similar ^{13}C NMR spectrum of glucose with the natural abundance distribution of ^{13}C with assignments (14). Comparison of Fig. 1 *a* and *b* shows that, to a high degree of accuracy, the ^{13}C label is observed mainly in

The publication costs of this article were defrayed in part by page charge payment. This article must therefore be hereby marked "*advertisement*" in accordance with 18 U. S. C. § 1734 solely to indicate this fact.

Abbreviations: αGP, L-glycerol 3-phosphate; DHAP, dihydroxyacetone phosphate; GAP, glyceraldehyde 3-phosphate; Fru-6-*P*, fructose 6-phosphate; Fru-P_2, fructose 1,6-bisphosphate; T3, L-3,3′,5-triiodothyronine.

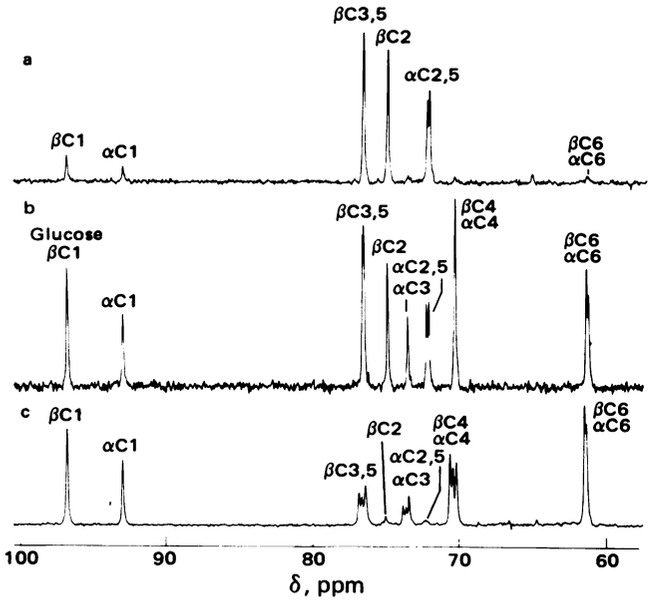

FIG. 1. ^{13}C NMR spectra at 25°C. (*a*) Liver cells from an euthyroid rat. This spectrum was measured during the period 68–105 min after the addition of 11 mM [2-^{13}C]glycerol. All labeled NMR peaks in this figure are due to glucose carbons. (*b*) ^{13}C NMR spectrum of glucose with the natural abundance distribution of carbon-13. (*c*) ^{13}C NMR spectrum taken 70–100 min after the addition of 22 mM (1,3-^{13}C]glycerol to a suspension of liver cells isolated from a rat treated with T3.

the C2 and C5 positions of glucose. Both of these positions can be traced back to the [2-^{13}C]glycerol label. Positions C4 and C6 of glucose, which cannot be traced back to the glycerol label, are decreased to less than 3% relative to the glucose C2 and C5 peaks. In cells from fasted rats, no glucose peaks are observed in the absence of labeled substrate (4).

Fig. 1*c*, showing the ^{13}C NMR spectrum of liver cells from hyperthyroid rats, was accumulated between 70 and 100 min after the addition of [1,3-^{13}C]glycerol. The ^{13}C distribution is as expected: there were intense and approximately equal peaks from the C1, C3, C4, and C6 sites of glucose whereas those from C2 and C5 were decreased to $\approx 1/10$th.

Changes of the concentration of [1,3-^{13}C]glycerol and αGP in hepatocytes from hyperthyroid rats with time are shown in Fig. 2. The lowfield regions showed the [1,3-^{13}C]glycerol peak decreasing with time, as did the αGP C1 and C3 peaks; at 85–115 min after glycerol introduction, both peaks, which previously had been intense, had disappeared. In a complementary fashion the glucose peaks increased rapidly and leveled off. The time courses of these peaks are plotted in Fig. 3, wherein cells from normal and hyperthyroid rats are compared. The hyperthyroid cells consumed glycerol 2 times faster than did cells from normal rats (Fig. 3*a*), and they had approximately one-third the level of αGP (Fig. 3*b*); also, they had a faster initial rate of glucose production, which leveled off as the glycerol was depleted (Fig. 3*c*).

Having emphasized the major pathways and the rate differences between normal and hyperthyroid rat liver cells, we turn to the information obtained from these spectra about the subsidiary pathways. Fig. 2 *inset*, from an experiment in which NH_4^+ and [1,3-^{13}C]glycerol were added to cells from a hyperthyroid rat, illustrates the upfield region, with increased gain, and shows the assignments of these peaks to specific carbons of different metabolites that are created from the glycerol precursor. These include lactate, alanine, β-hydroxybutyrate, acetoacetate, glutamate, and aspartate, all of which are close to the tricarboxylic acid cycle in the metabolic pathway.

In ^{13}C NMR spectra of liver cells from hyperthyroid rats,

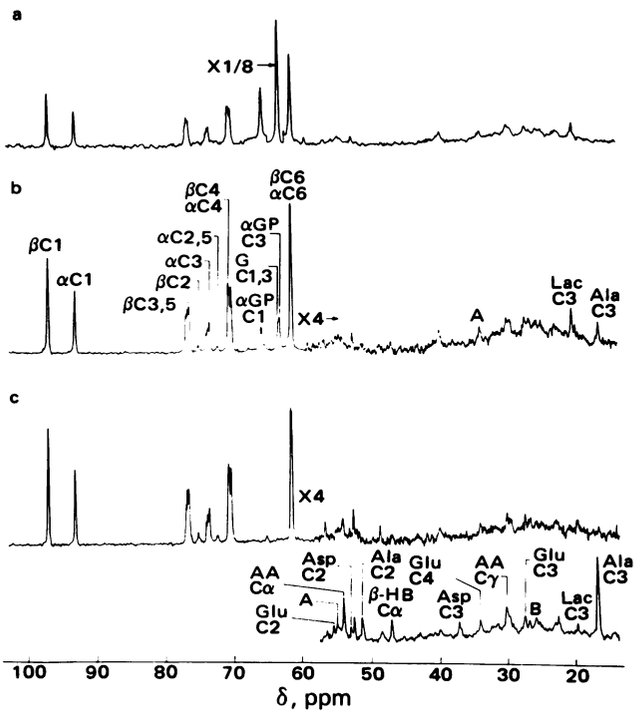

FIG. 2. Part of a sequence of ^{13}C NMR spectra at 25°C taken after a suspension of liver cells isolated from a T3-treated rat was made 22 mM in [1,3-^{13}C]glycerol. (*a*) Accumulated during the period 0–17 min after the addition of substrate; (*b*) 35–51 min; (*c*) 85–115 min. The pulse repetition rate was 0.334 sec for spectra *a* and *b* and 2 sec for spectrum *c*. (*Inset at bottom*) Upfield region of a similar hepatocyte sample made 16 mM in NH_4^+; recorded with increased vertical gain. The abbreviations used include: G C1,3, glycerol C1 and C3; αGP C1, α-glycerophosphate C1; Glu C2, glutamate C2; Asp C2, aspartate C2; AA Cα, acetoacetate CH_2; β-HB Cα, β-hydroxybutyrate CH_2; AA Cγ, acetoacetate CH3; and Lac C3, lactate C3.

suitably labeled lactate and alanine are seen at easily detectable levels in the presence or absence of exogenous NH_4^+. The time courses of glycerol consumption and glucose, lactate, and alanine levels in cells from hyperthyroid rats with and without added NH_4^+ are plotted in Fig. 4. The time course of αGP consumption was not affected by NH_4^+. The rates of glycerol use and glucose production were lower in the presence of added NH_4^+, and the production of labeled alanine was much greater when NH_4^+ was added. As Fig. 2 *inset* showed, the levels of ^{13}C-labeled aspartate, glutamate, and ketone bodies also were enhanced in the presence of NH_4^+. In the corresponding spectra

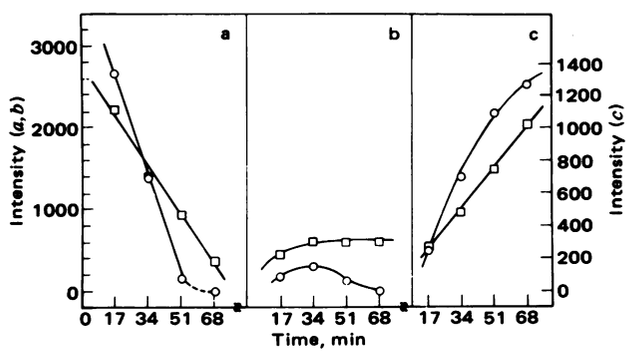

FIG. 3. Time course of glycerol consumption (*a*), αGP production and disappearance (*b*), and glucose production (*c*). Suspensions of liver cells from euthyroid (□) or hyperthyroid (○) rats were initially 22 mM in [1,3-^{13}C]glycerol. Each curve is the average of results from three animals. (*a*) Normalized intensity of the peak due to glycerol C1 and C3. (*b*) Normalized intensity of the C1 peak of αGP. (*c*) Intensity of the peak due to αC6 and βC6 of glucose.

of cells from euthyroid rats, however, lactate, alanine, other amino acids, and the ketone bodies have consistently been below our level of detection. These observations suggest a net increase in glycolytic end products in the cells from the hyperthyroid rats and are consistent with, e.g., the increased activity of lactate dehydrogenase (15) measured in thyroxine-treated rats.

Fig. 5*b* shows an enlarged portion of the glucose region of the spectrum shown in Fig. 2*c*. The multiplet structure observed comes from spin–spin interaction between the ^{13}C whose resonance is being observed and a ^{13}C near-neighbor in the same molecule. The outer doublets of each triplet shown in Fig. 5 are due to a ^{13}C-labeled C3(C4) of glucose split by its ^{13}C-labeled C4(C3) neighbor—both residing on the same molecule of glucose. The center member of each triplet is due to a ^{13}C-labeled C3(C4) of glucose adjacent to an unlabeled $^{12}C4$(C3) in that molecule. NMR spectra of the extracts gave a coupling constant $J_{3,4} = 38.71 \pm 0.01$ Hz. The heavy atom effect upon the chemical shifts is shown by the results $\delta(^{13}C4$ next to $^{12}C3) = 70.730$ ppm and $\delta(^{13}C4$ next to $^{13}C3) = 70.713$ ppm, so that the difference is 0.017 ppm. On the other hand, $\delta(^{13}C3)$ is the same next to $^{13}C4$ and $^{12}C4$. The observed C4 "heavy atom" shift is the same direction as most reported shifts of this sort (16). The chemically synthesized ^{13}C-labeled glycerol administered to the cells contained approximately 81% doubly labeled [1,3-^{13}C]glycerol; singly labeled [^{13}C]glycerol and unlabeled glycerol comprised the balance. The center line of the triplet should increase in intensity as the supply of unlabeled triose is increased. This is shown clearly in Fig. 5*a* in which 8 mM fructose (unlabeled) was added along with 22 mM [1,3-^{13}C]-glycerol to a suspension of hepatocytes from a hyperthyroid rat. The ratio of the integrated intensity of the C4 center line to the

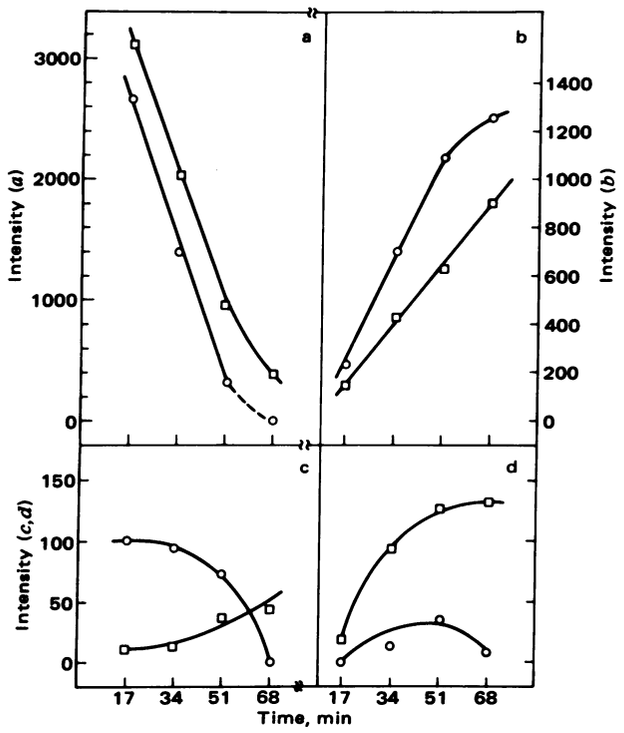

FIG. 4. Time course for glycerol consumption (*a*), glucose production (*b*), and lactate (*c*) and alanine (*d*) production and disappearance in hepatocytes isolated from hyperthyroid rats. The cell suspensions were initially either 22 mM in [1,3-^{13}C]glycerol (○) or 22 mM in [1,3-^{13}C]glycerol and 16 mM in NH_4^+ (□). Each curve is the average of results from two animals. All intensities are normalized to the same scale. (*a*) Intensity of the NMR peak due to glycerol C1 plus C3. (*b*) Peak due to αC6 and βC6 of glucose. (*c*) Lactate C3 peak. (*d*) Alanine C3 peak.

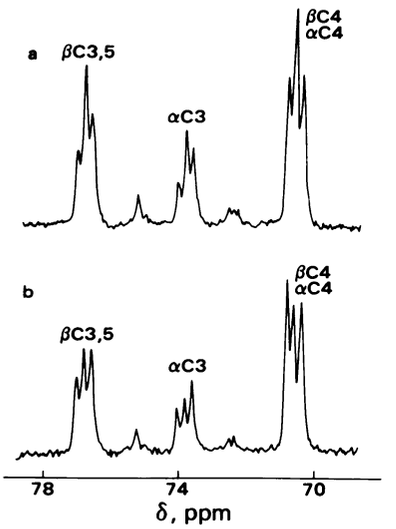

FIG. 5. (*a*) Expansion of the glucose C3 and C4 region of ^{13}C NMR spectrum of a suspension of liver cells from a rat treated with T3. The spectrum was accumulated 70–100 min after the addition of 22 mM [1,3-^{13}C]glycerol and 8 mM unlabeled fructose. (*b*) Expansion of the glucose C3 and C4 region of Fig. 2*c*.

integrated intensity of the outer C4 doublet is 0.17 in the absence of fructose and 0.50 in the presence of fructose, independent of time. From these data and the theoretical expression for this ratio, derived by taking into account the ^{13}C distribution at the triose level, we estimate that 22% of the flux into glucose came from unlabeled fructose. Another important experimental result is that, to within experimental error, the proportions of labeled and unlabeled neighbors were the same for C3 and C4.

DISCUSSION

The major pathway of ^{13}C-labeled glycerol into αGP and glucose is shown in Fig. 6. As mentioned briefly above, these pathways are consistent with the major labeling observed in all of our spectra. For example, Fig. 1*a* shows that when [2-^{13}C]-glycerol is used the most intense glucose peaks are those from the C2 and C5 carbons, just as expected, whereas Fig. 1*c* shows that [1,3-^{13}C]glycerol labels glucose strongly at C1, C3, C4, and C6. Furthermore, as shown in Fig. 2 for [1,3-^{13}C]glycerol (and in unpublished spectra for [2-^{13}C]glycerol), the labeled peaks of αGP can also be traced directly from the glycerol label. Beyond this first-order agreement with expectation, which accounts for ≈90% of the ^{13}C incorporated into glucose, there are three interesting results that can be obtained from the quantitative areas of the NMR peaks.

First, it is worth emphasizing that these ^{13}C NMR measurements give information not only about the percentage label at a particular carbon, such as could also be obtained by an analogous ^{14}C experiment, but also give the distribution of labeled carbons in the same molecule from the C3–C4 coupling. As discussed above, the center line of the C4 triplet measures the unlabeled trioses incorporated into glucose relative to the labeled trioses which are measured by the outer doublet. Hence, a single spectrum measures contributions from both labeled and unlabeled triose sources and can be interpreted to give total from glucose production triose as well as determining the label concentration.

Second, as given in Table 1, the C4/C3 intensity ratio was 1.00 ± 0.03 in all our spectra when glycerol was the substrate, showing that the labeled flux into glucose had equal contributions from the two trioses dihydroxyacetone phosphate (DHAP) and glyceraldehyde 3-phosphate (GAP). The same conclusion

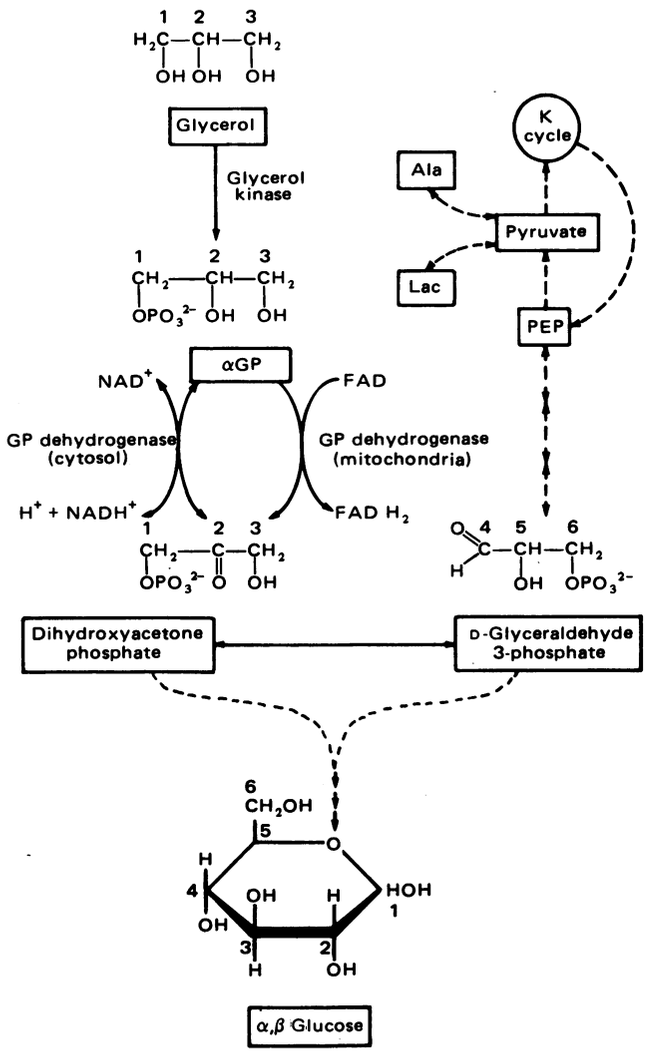

FIG. 6. Gluconeogenic pathway from glycerol. K cycle, Krebs (tricarboxylic acid) cycle; PEP, phospho*enol*pyruvate.

can be drawn from the multiplet spectra of Fig. 5, in which the C3 neighbors of C4 had the same fractional ^{13}C composition as did the C4 neighbors of C3. Because glycerol feeds directly into DHAP, simple explanations of this fact are either that triose phosphate isomerase, which catalyzes the DHAP $\rightleftharpoons$ GAP interconversion, is at equilibrium or, alternatively, that there is no detectable unlabeled flux into the GAP pool. One could distinguish between these possibilities by introducing a nonlabeled flux into GAP that is comparable to the labeled flux coming into DHAP from glycerol.

Third, these data can be used to determine the flux in liver cells through the pentose cycle. In Fig. 1*a* the glucose peaks

Table 1. Distribution of ^{13}C in glucose formed from ^{13}C-labeled glycerol by isolated hepatocytes

	From [1,3-^{13}C]glycerol*	From [2-^{13}C]glycerol†
C4/C3	1.00 ± 0.03	
C6/C1	1.13 ± 0.03	
C5/C2		1.10 ± 0.03
C1/C5		0.14 ± 0.04

Results are expressed as the mean ± SD for the ratio of the integrated intensities of the designated glucose lines. All data are from spectra recorded under nonsaturating conditions at a point in the experiment when all glycerol had been consumed.
* Average for three euthyroid control and four T3-treated rats.
† Average for two euthyroid and two T3-treated rats.

directly traceable to [2-^{13}C]glycerol are due to C2 and C5 and all are very intense. The βC1 and αC1 peaks, however, have intensities significantly above the natural abundance level and, furthermore, are quite sharp, indicating that the adjacent C2 is unlabeled. Enrichment of ^{13}C at C1 in glucose with concomitant loss of ^{13}C at the directly labeled C2 position and without enrichment at C4 or C6 can occur *in vivo* during cycling through the pentose pathway. The relative ^{13}C enrichment at C6 compared with C1, when the substrate was [1,3-^{13}C]glycerol, taken together with the equal flux of the triose units into glucose, indicates a loss of labeled C1 as $^{13}CO_2$ in the oxidative pentose phosphate pathway. Hence, we should observe a loss of label at C2 relative to C5. Fig. 1*a* and the data in Table 1 show that this is exactly what is observed; all these data are consistent with ≈10% pentose cycle activity.

In addition to the estimation of total flux through the pentose cycle, the low level of labeling at C3 (Fig. 1*a*) and the equal labeling at C3 and C4 (Table 1) give information that can be used to determine the relative activities of the transaldolase (TA) and transketolase (TK) reactions, which have three parts (17) symbolized by

$$P + P \overset{TK}{\rightleftharpoons} GAP + S \quad [1]$$

$$GAP + S \overset{TA}{\rightleftharpoons} E + \text{Fru-6-}P \quad [2]$$

$$E + P \overset{TK}{\rightleftharpoons} GAP + \text{Fru-6-}P \quad [3]$$

in which P denotes either xylulose or ribose 5-phosphate, S is sedoheptulose 7-phosphate, E is erythrose 4-phosphate, and Fru-6-*P* is fructose 6-phosphate. The sum of these reactions is

$$3P \rightleftarrows GAP + 2\text{Fru-6-}P.$$

Following all or part of the reaction scheme of Eqs. 1–3, we consider two simplified pathways, of which one is capable of explaining our observations and is consistent with previous ^{14}C studies (18–20) of the pentose cycle. We assume that (*i*) all of the flux through the oxidative pentose path is returned to hexoses [i.e., the purpose of the cycle under our conditions is to regenerate NADPH, and no pentoses are created in the nonoxidative pathway (because none are observed)]; (*ii*) the TK reactions may have appreciable rates in both directions whereas the TA reaction is essentially irreversible; and (*iii*) the pentoses are all in equilibrium. Finally, we illustrate the effects of two extreme pathways and disregard the complicated interactions among their intermediates, which do in some cases make up common pools.

With these assumptions we describe the scrambling of the hexose label expected under two conditions, illustrating them by following the 2,5-^{13}C-labeled hexose.

Pathway 1. Three pentoses formed in the oxidative path, accordingly now [1,4-^{13}C]P, go through Eqs. 1–3 irreversibly and form two hexoses: [1,3,5-^{13}C]Fru-6-*P* and [1,5-^{13}C]Fru-6-*P*.

Pathway 2. As assumed above (*ii*), the TK reactions are reversible, with a rate on the order of the pentose cycle rate, and affects the hexose ^{13}C label distribution in two different ways (whereas the TA reaction is unidirectional): TK exchange can convert 1,4-^{13}C-labeled pentoses into hexoses, and it must, according to assumption *i*, return an equal amount of hexoses to the pentose pool as 2,4-^{13}C-labeled pentoses. The first of these will create 1,5-^{13}C-labeled hexoses. The second will create 2,4-^{13}C-labeled pentoses, three of which must be consumed by Eqs. 1–3 to form a [2,5-^{13}C]Fru-6-*P* and a [2,3,5-^{13}C]Fru-6-*P*.

Table 2. Observed and calculated ^{13}C distributions in glucose formed from ^{13}C-labeled glycerol

	Observed	Expected: Unidirectional flow through TA and TK (Eqs. 1–3, pathway 1)*	Expected: Pathway 2*
[2-^{13}C]Glycerol $\alpha C1/\alpha C3$	2.9 ± 0.4	1.9	2.2
[1,3-^{13}C]Glycerol C2 multiplet structure	1:1.8:1	1:3.3:1†	1:1.9:1†

* Values calculated for 10% pentose cycle contribution.

† The center line of each multiplet includes contributions that are due to the presence of unlabeled and singly labeled glycerol in the substrate (as described in the text) and also a contribution due to the presence of glucose with the natural abundance distribution of ^{13}C at C2.

The $\alpha C1/\alpha C3$ ratios expected from these two models are compared with the observed ratios in the first row of Table 2. Pathway 1 gives a value that is smaller than the observed value whereas pathway 2 gives a value closer to that observed. When both the TA and TK reactions are rapidly reversible, the C1/C3 ratio, according to the computer calculation by Katz and Rognstad (19), is much lower than that observed. The ^{13}C NMR spectra give not only the percentage label at C2 in the [1,3-^{13}C]glycerol experiment but also the distribution of label within the same glucose molecule from the C2–C3 coupling seen in the outer doublet of the C2 triplet. Fitting the multiplet ratios observed at C2 thus provides a stringent test of the model pathway. The second row of Table 2 shows that pathway 2 fits the observed C2 ratios well.

Another general area investigated by these experiments concerns the effects of T3 treatment upon glycerol metabolism. Previous reports (5, 8) of increased gluconeogenic rates from glycerol in hepatocytes from thyroxine-treated rats are supported by the faster glycerol consumption and glucose production shown in Fig. 3 *a* and *c*, respectively. Fig. 3*a* allows us to calculate that the rate of glycerol consumption is 2 times faster after T3 treatment; Fig. 3*b* shows that in the hyperthyroid state the αGP concentration is 40% of normal. Using the detritiation of [2-^{3}H]αGP by isolated liver mitochondria, Carnicero *et al.* (21) determined that the K_m of the mitochondrial αGP dehydrogenase is 5-fold greater in the hyperthyroid state, whereas V_{max} is 16-fold greater. From Fig. 3 we estimate the intracellular concentration of αGP to be 7.5 and 17 mM in our hyperthyroid and normal cells, respectively. We estimate that in our T3-treated cells 40% of the αGP is oxidized by the cytosolic enzyme and 60% is oxidized by the mitochondrial dehydrogenase; in our euthyroid cells these values are 85 and 15% for the cytosolic and mitochondrial enzymes, respectively. In agreement with these estimates for normal cells is the finding by Carnicero *et al.* (21) that, in perfused euthyroid liver, rotenone (which blocks only the cytosolic enzyme) decreases the rate of detritiation of αGP produced from [2-^{3}H]glycerol to 20% of the control rate. In agreement with our estimate for cells from T3-treated rats is the measurement by Werner and Berry (8) that, in cells from hyperthyroid rats, 58% of the hydrogen flux to O_2 during glycerol metabolism uses an antimycin-sensitive, rotenone-insensitive pathway, presumably the mitochondrial αGP dehydrogenase.

Table 1 shows no significant difference between normal and hyperthyroid rats for any of the ratios given. It is known that in hyperthyroid rats the activities of two enzymes of the oxidative pentose pathway are increased 2-fold (15, 22) and that liver DNA synthesis is increased 10 to 30-fold (23); however, our spectra would not reveal an increased flow of ribose into biosynthetic pathways.

The NMR method has the advantage of simultaneously detecting all metabolites that have been adequately labeled. For example, spectra of T3-treated cells revealed the glycolytic end products lactate and alanine while we were studying gluconeogenesis from glycerol. Furthermore, when NH_4^+ was added to the T3-treated cells, quite high levels of alanine, aspartate, glutamate, and ketone bodies were observed, reflecting increased flux through the tricarboxylic acid cycle during active gluconeogenesis.

S.M.C. was supported by a Fellowship Grant from the American Cancer Society (PF-1365) and is the holder of the American Association of University Women Inez Shaefer Fellowship.

1. Ugurbil, K., Rottenberg, H., Glynn, P. & Shulman, R. G. (1978) *Proc. Natl. Acad. Sci. USA* **75**, 2244–2248.
2. Ugurbil, K., Brown, T. R., den Hollander, J. A., Glynn, P. & Shulman, R. G. (1978) *Proc. Natl. Acad. Sci. USA* **75**, 3742–3746.
3. Cohen, S. M., Ogawa, S., Rottenberg, H., Glynn, P., Yamane, T., Brown, T. R. & Shulman, R. G. (1978) *Nature (London)* **273**, 554–556.
4. Cohen, S. M., Ogawa, S. & Shulman, R. G. (1978) in *Frontiers of Biological Energetics*, eds. Dutton, P. L., Leigh, J. & Scarpa, A. (Academic, New York), Vol. 2, pp. 1357–1364.
5. Freedland, R. A. & Krebs, H. A. (1967) *Biochem. J.* **104**, 45.
6. Woods, H. F. & Krebs, H. A. (1973) *Biochem. J.* **132**, 55–60.
7. Burch, H. B., Lowry, O. H. Meinhardt, L., Max, P., Jr. & Chyu, K. J. (1970) *J. Biol. Chem.* **245**, 2092–2102.
8. Werner, H. V. & Berry, M. N. (1974) *Eur. J. Biochem.* **42**, 315–324.
9. Berry, M. N., Kun, E. & Werner, H. V. (1973) *Eur. J. Biochem.* **33**, 407–417.
10. Lee, Y. P., Takemori, A. E. & Lardy, H. (1959) *J. Biol. Chem.* **234**, 3051–3054.
11. Berry, M. N. & Friend, D. S. (1969) *Cell Biol.* **43**, 506–520.
12. Tischler, M. E., Hecht, P. & Williamson, J. R. (1977) *Arch. Biochem. Biophys.* **181**, 278–292.
13. Ogawa, S., Shulman, R. G., Glynn, P., Yamane, T. & Navon, G. (1978) *Biochim. Biophys. Acta* **502**, 45–50.
14. Stothers, J. B. (1972) *Carbon-13 NMR Spectroscopy* (Academic, New York), p. 461.
15. Freedland, R. A. (1965) *Endocrinology* **77**, 19–27.
16. Batiz-Hernadez, H. & Bernheim, R. A. (1967) in *Progress in Nuclear Magnetic Resonance Spectroscopy*, eds. Emsley, J. W., Feeney, J. & Sutcliffe, L. H. (Pergamon, Oxford), Vol. 3, pp. 63–85.
17. Stryer, L. (1975) *Biochemistry* (W. H. Freeman, San Francisco), pp. 356–365.
18. Rognstad, R. & Katz, J. (1976) *Arch. Biochem. Biophys.* **177**, 337–345.
19. Katz, J. & Rognstad, R. (1967) *Biochemistry* **6**, 2227–2247.
20. Rognstad, R. (1976) *Int. J. Biochem.* **7**, 221–228.
21. Carnicero, H. H., Moore, C. L. & Hoberman, H. D. (1972) *J. Biol. Chem.* **247**, 418–426.
22. Young, J. W. (1968) *Am. J. Physiol.* **214**, 378–383.
23. Short, J., Brown, R. F., Husakova, A., Gilbertson, J. R., Zemel, R. & Lieberman, I. (1972) *J. Biol. Chem.* **247**, 1757–1766.